PAPER • **OPEN ACCESS**

Numerical calculation of the loss resistance of VLF monopole antennas using the equivalent conductivity of the ground plane

View the article online for updates and enhancements.

Numerical calculation of the loss resistance of VLF monopole antennas using the equivalent conductivity of the ground plane

Bin Li[1,*], Chao Liu[1] and Yanshi Li[2]

[1]Department of Electronic Engineering, Naval University of Engineering, Wuhan, China
[2]Shandong Zhongji Geoinformation and Technology Company Limited, Jinan, China

*Corresponding author e-mail: libin521002@sina.com

Abstract. In this study, the ground-loss resistances of very low frequency (VLF) monopole antennas are considered. A novel method of obtaining solutions of the magnetic field and electric field losses for the earth system is outlined. The equivalent conductivity of the ground system is obtained using the parallel relationship between the nature surface and the ground wires. This provides significant convenience for the calculation of the ground loss and the design of the ground system. Because an equivalent ground plane is used, a unique solution of the ground loss resistances is achieved by using the integral of the equivalent unit circles. The proposed method is verified by comparing the numerical integral method and full-wave simulations. The numerical results and the effects of the VLF monopole antenna configurations on the loss resistances for different monopole heights and artificial-ground-plane installations are discussed.

1. Introduction
A ground system consisting of a radial wire grid has been proven an effective approach for improving antenna performance [1-3]. Two types of power losses occur in ground systems, i.e., the magnetic field loss that is caused by induced currents due to imperfect ground conductivity and the electric field loss that is caused by a displacement current through the ground plane [4-6]. Due to the requirement of good ground conductivity, ground loss resistance is one of the most important parameters for assessing the performance of a very low frequency (VLF) array in different configurations, i.e., top-load structure (umbrella and inverted core, etc.) [7-9]. The design of a complex ground screen and the determination of the loss resistances are important factors for obtaining high radiation efficiency.

Many advanced calculation methods have been presented during the past several decades. For an electrical small antenna (ESA) with an earth system, the analytic solutions of the impedances and radiation patterns have been evaluated and proved by Wait [10]. Simplified calculations of ground loss for a monopole antenna were implemented in [11] and this was followed by an accurate evaluation based on Joule's law in [12]. Vainstein's theorem was employed for the ground-loss calculation in [13]. Despite the development of suitable analytic expressions, they tend to simplify the ground screen as a homogenous radial wire or a thin metallic layer, which results in a relatively inefficient design, especially when multiple segmented wires are required in VLF vertical antennas. At present, the method of moments (MoM) is widely applied due to developments in computational performance [14-

16]. Commercial software based on the MoM can provide simulation values for the loss resistance [17]. However, for a VLF ground system with a large antenna structure, the solutions of the loss resistances are non-unique and there are large differences because of the variable mesh size in the MoM method [18, 19]; this results in a lack of reliability. In this study, a novel method is proposed for calculating the loss resistances of VLF grounded monopole antennas. The proposed method differs from the previously used analytic methods. We extract an equivalent solution of the original ground system by introducing the concept of equivalent conductivity of the ground plane. The artificial ground plane (AGP) is transformed into a finite conductivity plane. Therefore, the ground loss resistances can be obtained by using the integral of the equivalent unit circles. The proposed method is not only suitable for a homogeneous wire grid but also performs well for a segmented wire ground screen.

The remainder of this paper is organized as follows: Section 2 describes the numerical calculations for determining the ground-loss resistances and the equivalent conductivity of the ground system. In Section 3, we present the numerical results of the ground loss resistances and illustrate the effects of the monopole antenna. The conclusions of this study are presented in Section 4.

2. Calculation method

As mentioned above, conduction currents affluxing along the earth surface and electromagnetic waves penetrating into the ground plane with finite conductivity contribute to power loss. The power loss of the vertical VLF antenna in the ground plane needs to be reduces by installing a ground system above the finite conducting plane. Let us consider a grounded monopole antenna with the ground screen of N perfect conducting radial wires. As shown in Fig.1, the monopole antenna with N ground wires is laid on the ground plane. The ground plane can be separated into two separate areas, i.e., an AGP and the soil plane. For an electric small VLF monopole antenna, the major ground loss is produced in the region of $\rho \leq \lambda / 2\pi$, where ρ denotes the distance between the monopole pedestal and the component angle of the magnetic field and the input current are in-phase. Therefore, the total power loss of the ground system is defined as [6]:

$$W_{\text{loss}} = W_A + W_N \tag{1}$$

where W_N and W_A denote the power losses of natural ground plane (NGP) and AGP respectively.
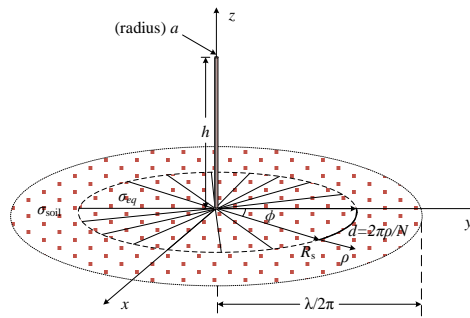

Figure 1. A grounded monopole antenna with a homogenous radial earth screen.

It is convenient to analyze the magnetic field losses and electric field losses for each region separately. The total power loss can be categorized into four parts: the AGP electric field loss, the NGP electric field loss, the AGP magnetic field loss, and the NGP magnetic field loss. For the monopole antenna, the tangential component of magnetic field $H_\varphi(\rho)$ and the vertical electric field E_z are defined respectively as follows [10]:

$$E_z = \frac{-I_0}{2\pi j\omega\varepsilon_0 h^2}[1 + (\rho / h_e)^2]^{-\frac{3}{2}} \tag{2}$$

$$H_\varphi(\rho) = \frac{I_0}{2\pi} \cdot \frac{h}{\sqrt{\rho(\rho^2 + h_e^2)}} \tag{3}$$

where $\omega = 2\pi f$ denotes the angle frequency, ε_0 denotes the permittivity, and h_e denotes the monopole antenna's effective height. To emphasize the property of the earth system, the characteristic admittance of the soil is expressed by [11]:

$$Y_s = \sqrt{(\varepsilon - \frac{j\sigma}{\omega}) / \mu} \tag{4}$$

where ε denotes the soil permittivity, σ denotes the soil conductivity, and μ denotes the permeability of the soil. The characteristic admittance of the inhomogeneous ground wire is defined as follows:

$$Y_g = -j / [f \mu d \ln(\frac{d}{2\pi a})] \tag{5}$$

where $d = 2\rho \sin(\pi/N) \approx 2\pi\rho / N$ denotes the inter-spacing of two adjacent ground wires and a denotes the radius of the ground wire. In the AGP, Y_s and Y_g are connected in series, which has been proven by Wait [10]. To elevate the conductivity of the AGP, we introduce the equivalent conductivity plane to cascade the ground wires grid and the natural soil. Therefore, the equivalent characteristics admittance of the AGP has the following form:

$$Y_{eq} = \sqrt{(\varepsilon - \frac{j\sigma(r)}{\omega}) / \mu}, 0 < r \le R_s \tag{6}$$

where $\sigma(r)$ denotes the AGP's equivalent conductivity and r denotes the distance between the monopole antenna pedestal and the grid-point. We recall that $Y_{eq} = Y_s + Y_g$. According to equations (4) ~ (6), the equivalent conductivity can be expressed as follows:

$$\sigma(r) = \sigma - \frac{\omega}{jf^2\mu d^2 \ln^2(\frac{d}{2\pi a})} + 2\omega\sqrt{(\varepsilon - j\frac{\sigma}{\omega}) / \mu} / (fd \ln\frac{d}{2\pi a}) \tag{7}$$

where

$$d = 2r \sin(\pi/N) \approx 2\pi r / N \tag{8}$$

Since our discussion focus on cases in the VLF band, where $\sigma \gg \omega\varepsilon$, equation (7) can be simplified as:

$$\sigma(r) = \frac{\sqrt{\frac{2\sigma\omega}{\mu}}}{fd \ln(\frac{d}{2\pi a})} + \sigma - j \cdot [\frac{2\pi}{f\mu d^2 \ln^2(\frac{d}{2\pi a})} + \frac{\sqrt{\frac{2\sigma\omega}{\mu}}}{fd \ln(\frac{d}{2\pi a})}] \tag{9}$$

The values of the equivalent resistivity as a function of r/λ are depicted in Figure 2 to obtain a comparison of different radial wires. In the radial wire grid, the conductivity of the AGP increases with the distance and approaches the natural ground resistivity; the conductivity is lower for larger numbers of ground wires, as expected. Under the conditions of $\sigma = 0.01 \, \text{S/m}$ and $f = 20 \, \text{kHz}$, the equivalent conductivity is larger than 0.05 S/m for $N = 300$ in most regions of the AGP.
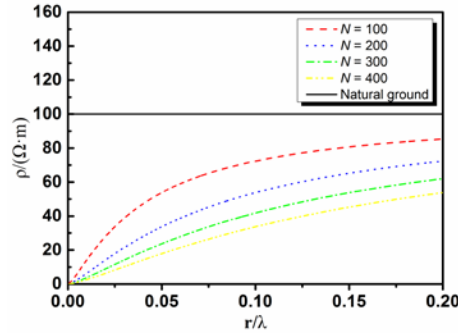
Figure 2. Equivalent resistivity of the AGP versus the radial distance.

Substituting equation (9) into equation (6) yields the equivalent admittance of the AGP. The AGP can be transformed into an equivalent ground plane with the conductivity of Y_{eq}. By separating the equivalent ground plane into m concentric rings, the total loss resistances of the ground system with segmented radial wire grids can be obtained by:

$$\begin{aligned}
R_{loss} &= R_E + R_H \\
&= \frac{2\pi}{I_0^2}(\sum_i \int_{r_i}^{r_{i+1}} R_{E_i}^{'} J_z^2 \rho \mathrm{d}\rho + \int_{R_s}^{\frac{\lambda}{2\pi}} R_E^{'} J_z^2 \rho \mathrm{d}\rho \\
&\quad + \sum_i \int_{r_i}^{r_{i+1}} R_{H_i}^{'} H_{\varphi}^2(\rho) \rho \, \mathrm{d}\rho + \int_{R_s}^{\frac{\lambda}{2\pi}} R_H^{'} H_{\varphi}^2(\rho) \rho \mathrm{d}\rho)
\end{aligned} \tag{10}$$

where $R_E^{'}$ and $R_H^{'}$ are the per unit area electric field and magnetic field loss resistances respectively, $r_i (i = 1, 2, \ldots, m)$ denotes the distance between the ith slip ring and the antenna pedestal, and $J_z = \omega \varepsilon_0 E_z$ denotes the conduction current density produced by E_z. Due to the inhomogeneous distribution of the near field, the inhomogeneous ground system performs better in terms of the reduction in power loss than the homogeneous ground system. The ground system can be optimized by using the analytical solution of the ground loss obtained by equation (10).

3. Numerical examples

In order to verify the effectiveness of the equivalent approach, the ground loss resistance of the monopole antenna in the AGP with the radius of 1600 m is calculated using Wait's method, the simulation software, and our proposed method. The height of the monopole antenna is 300 m. The AGP of the monopole antenna consists of 100 grounding wires with an angle of 3.6°. Three slip rings are set at the radial distance of 400 m, 1200 m, and 1600 m, respectively. The radius of the wires is 0.0015 m. The conductivity of the ground is 0.01 S/m. The mesh size of the AGP is λ/600.

As shown in Table 1, the calculated values of the ground loss resistance are qualitatively consistent using the analytical values derived from Wait's method. The calculated solutions of the loss resistance are 7.59% higher than the simulation values of the model at the same frequency. The electric field loss accounts for 2.18% of the total loss. It is essential to note that the simulation results are mostly unequal for the different mesh sizes.

Table 1. Ground loss resistance results.

Frequency/kHz	magnetic field loss/mΩ	electric field loss/mΩ	Total loss/mΩ	Wait's method/mΩ [10]	Simulation values/mΩ
20	52.43	1.31	53.74	55.01	50.89
21	55.08	1.31	56.39	57.82	52.25
22	57.64	1.31	58.95	60.62	54.77
23	60.24	1.31	61.55	63.42	57.03
24	62.86	1.31	64.17	66.21	59.33
25	65.49	1.31	66.80	68.99	61.66

3.1. *Ground loss resistances for different monopole heights*

In this section, we focus on the effect of the monopole height on the loss resistances of the monopole antenna. A homogenous segmented AGP with radial wires is installed on the surface.
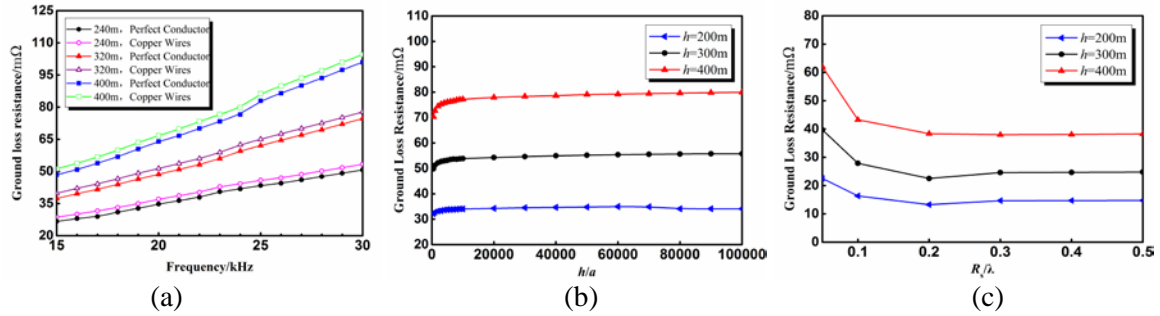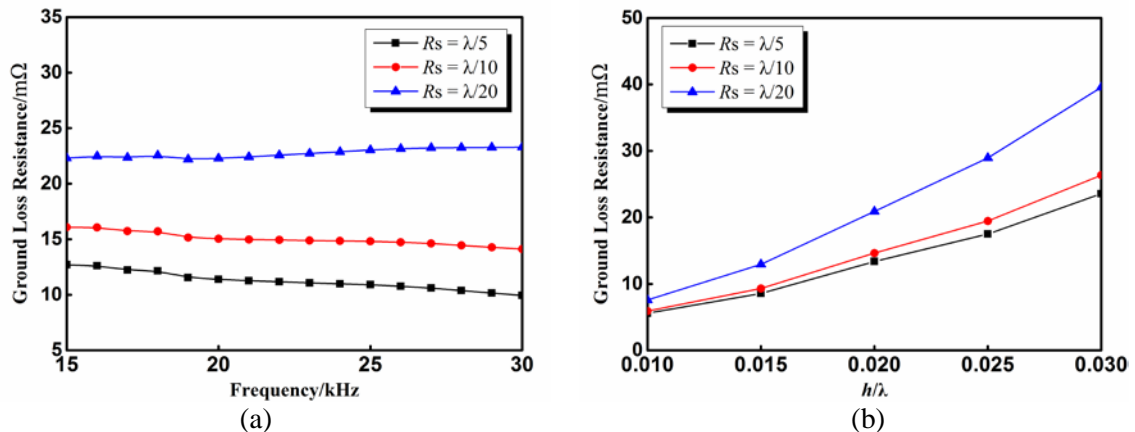

(a)   (b)   (c)

Figure 3. The ground loss resistances of the VLF monopole antenna with different monopole heights (a) The loss resistances versus frequency ($N = 100$, $Rs = \lambda / 10$, $a = a_0 = \lambda / (5 \times 10^6)$, $\sigma = 0.01 \, \text{S/m}$, $\varepsilon_r = 20$, $\sigma_{\text{copper}} = 5.8 \times 10^7 \, \text{S/m}$). (b) The loss resistances versus the antenna's ratio of h / a ($f = 25 \, \text{kHz}$, $N = 100$, $Rs = 1600 \, \text{m}$, $a_0 = 0.0015 \, \text{m}$, $\sigma = 0.01 \, \text{S/m}$, $\varepsilon_r = 20$). (c) The loss resistances versus the radius of the AGP ($f = 25 \, \text{kHz}$, $N = 200$, $h / a = 1 \times 10^5$, $a_0 = 0.0015 \, \text{m}$, $\sigma = 0.01 \, \text{S/m}$, $\varepsilon_r = 20$).

Figure 4(a) presents the ground loss resistances are increasing more rapidly with increasing frequencies for the larger monopole heights. The monopole height clearly increases the ground loss resistance. The loss resistances of the copper wires are 6.29% higher than the loss resistances of the perfect electric conductor (PEC). There is a negligible influence of the frequency on the increment of the loss resistances in the VLF band. Figure 4(b) shows the relationship between the ground loss resistances and the ratio of h / a with different monopole heights at 25 kHz. As the ratio of h / a is larger than 10000, both resistances are independent of the ratio. However, for the monopoles with $h = 300 \, \text{m}$ and $h = 400 \, \text{m}$, both resistances increase slightly with increasing the ratio of h / a at a low ratio. In Figure 4(c), the ground loss resistances are presented as the growing radius of the AGP for different antenna heights. Within a radius of 0.2λ, the ground loss resistances decrease as the radius of the AGP increases. Because the magnetic field and electric field losses are mainly focused on the pedestal of the monopole antenna. It is observed that the ground loss resistance does not change much when the radius of the AGP exceeds 0.2λ.

3.2. *Ground loss resistances for different AGP installation*s

In this section, the ground loss resistances for different AGP installations are calculated in detail. To control the study variables, we retain the other electrical parameters of the model. The ground loss resistances are shown in Figure 4.
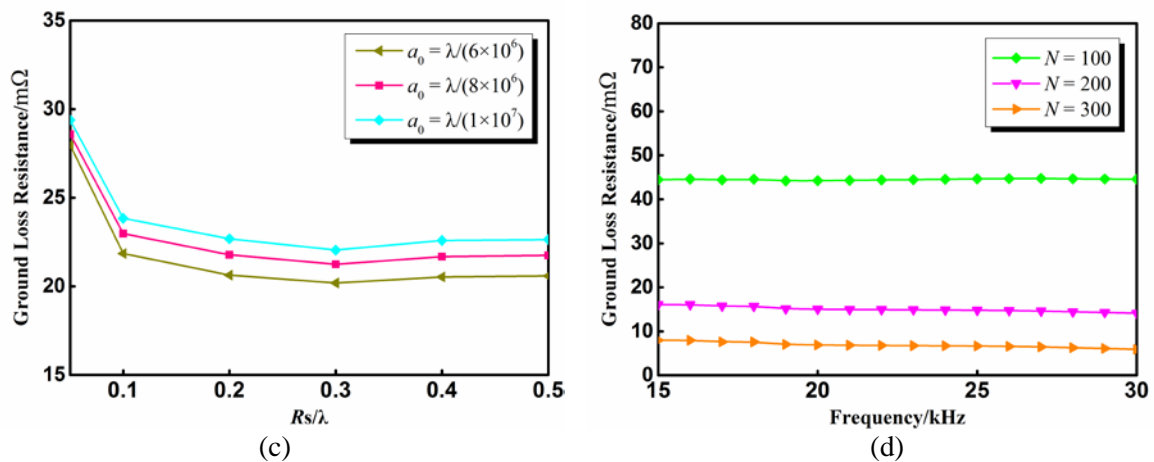

(a)   (b)

Figure 4. The ground loss resistances of the VLF monopole antenna with different AGP installations. (a) The loss resistances versus the frequency with different radii of the AGP ($N = 200$, $h = 0.02\lambda$, $h / a = 1 \times 10^5$, $a_0 = \lambda / (1 \times 10^7)$, $\sigma = 0.01 \mathrm{S/m}$, $\varepsilon_r = 20$). (b) The loss resistances versus the monopole height with different radii of the AGP ($f = 25 \mathrm{kHz}$, $a = 0.006 \mathrm{m}$, $N = 200$, $a_0 = 0.0015 \mathrm{m}$, $\sigma = 0.01 \mathrm{S/m}$, $\varepsilon_r = 20$). (c) The loss resistances versus the AGP radius ($f = 25 \mathrm{kHz}$, $N = 200$, $h = 0.02\lambda$, $h / a = 1 \times 10^5$, $\sigma = 0.01 \mathrm{S/m}$, $\varepsilon_r = 20$). (d) The loss resistances versus the frequency with different ground wire numbers ($Rs = \lambda / 10$, $h = 0.02\lambda$, $h / a = 1 \times 10^5$, $a_0 = \lambda / (1 \times 10^7)$, $\sigma = 0.01 \mathrm{S/m}$, $\varepsilon_r = 20$).

Figure 4(a) depicts the ground loss resistance of the VLF monopole versus the frequency with different AGP's radii. As expected, the loss resistance remains a constant for the same electrical parameters. The frequencies in the VLF band have little effect on the ground loss resistances of the monopole antenna. We observe that the resistances are larger for the longer ground wires as the equivalent conductivities of the ground plane are larger. Figure 4(b) clearly shows that the ground loss resistances increase with the increase in the height of the monopole antenna. As the monopole antenna height increases, the ground loss resistances are larger for the AGP with longer radial wires. Figure 4(c) shows that the ground loss resistances decrease with the increase in the radius of the AGP for different wire radii., The ground loss resistances are slightly lower for the monopole antenna with $a_0 = \lambda / (6 \times 10^6)$ than for the antenna with $a_0 = \lambda / (1 \times 10^7)$ for the same AGP radius. Figure 4(d) presents the ground loss resistances as functions of the frequency for different number of wires. It is observed that the larger the number of wires is, the lower the ground loss resistances are. However, there was no significant difference in the ground loss between 200 and 300 radial wires.

4. Conclusions

In this study, the loss resistance of an AGP for a VLF monopole antenna is investigated. A novel method based on the equivalent conductivity of the AGP is proposed. Unlike the simulation methods, the ground loss values obtained by the proposed method have a unique solution. Moreover, the proposed method is also applied to analyze the ground loss resistances of a segmented ground screen. The ground loss resistances of the VLF monopole antenna are calculated in detail for different monopole heights and AGP installations. Future work in this area will include optimizing the ground screen by varying the number of segments in the ground screen, and calculating the ground loss resistance of a monopole antenna with a large top load.

Acknowledgments

References

[1] M. Fartookzadeh, S. H. M. Armaki, S. M. J. Razavi, et al., Optimum functions for radial wires of monopole antennas with arbitrary elevation angles, Radioeng. 25 (2016) 53-60.

[2] H. Rmili, L. Aberbour, C. Craeye, On the radiation resistance of a planar monopole antenna with reduced groundplane, IEEE Antennas Wireless Propagat. Lett. 9 (2010) 732-736.

[3] B. A. Austin, A. Boswell, and M. A. Perks, Loss mechanisms in the electrically small loop antenna [antenna designer's notebook], IEEE Antennas Propagat. Mag. 56 (2014) 142-147.

[4] V. Trainotti and L. A. Dorado, Short low- and medium-frequency antenna performance, IEEE Antennas Propagat. Mag. 47 (2005) 66-90.

[5] V. Trainotti and G. Figueroa, Vertically polarized dipoles and monopoles, directivity, effective height and antenna factor, IEEE Trans. Broadcast. 56 (2010) 379-409.

[6] G. L. Dai and Y. H. Dong, Calculation and analysis of ground loss resistance for an electrically small VLF transmitting antenna, Chin. J. of Radio Sci. 33 (2018) 483-489.

[7] B. Li, C. Liu, H. Wu, A moment-based study on the impedance effect of mutual coupling for VLF umbrella antenna arrays, Prog. Electromagn. Res. C. 76 (2017) 75-86.

[8] H. F. Li and C. Liu, "Calculation on characteristics of VLF umbrella inverted-cone transmitting antenna," in 2014 Sixth International Conference on Ubiquitous and Future Networks (ICUFN), IEEE, Shanghai, China, 2014, pp. 389-391.

[9] R. Kichouliya, P. Kumar, S. M. Satav, et al., Electromagnetic Field Coupling to Large Antenna Structure, Prog. Electromagn. Res. M. 73 (2018) 9-16.

[10] J. R. Wait, Antenna Performance Influenced by the Finite Extent and Conductivity of Ground Planes: A Collection of Reprints, No. M90-79., Mitre Corp., Bedford, 1990.

[11] L. A. Dorado, V. Trainotti, Simplified calculation of ground losses in low and medium frequency antenna systems, IEEE Antennas Propagat. Mag. 48 (2006) 70-81.

[12] L. A. Dorado, V. Trainotti, Accurate evaluation of magnetic- and electric-field losses in ground systems, IEEE Antennas Propagat. Mag. 49 (2007) 58-70.

[13] B. Levin, "Resistance of losses in the earth," in 2015 IEEE International Seminar/Workshop on Direct and Inverse Problems of Electromagnetic and Acoustic Wave Theory (DIPED), IEEE, Lviv, Ukraine, 2015, pp. 45-48.

[14] B. Li, C. Liu, Y. H. Dong, Spatial power combining of VLF umbrella antenna arrays with multi-delay lines, Prog. Electromagn. Res. C. 80 (2018) 79-87.

[15] K. Alkhalifeh, G. Hislop, N. A. Ozdemir, et al., Efficient MoM simulation of 3-D antennas in the vicinity of the ground, IEEE Trans. Antennas Propagat. 64 (2016) 5335-5344.

[16] H. T. Chou, H. K. Ho, Local area radiation sidelobe suppression of reflector antennas by embedding periodic metallic elements along the edge boundary, IEEE Trans. Antennas Propagat. 65 (2017) 5611-5616.

[17] Amiri, M. A., C. A. Balanis, C. R. Birtcher, "Analysis, design, and measurements of circularly symmetric high-impedance surfaces for loop antenna applications," IEEE Trans. Antennas Propagat. 64 (2016) 618-629.

[18] A. Sawitzki, Electromagnetic modelling of surfaces using method of moments with calculated phase mesh, IET Microw. Antennas Propagat. 9 (2015) 1354-1362.

[19] Huang, K., Y. Y. Li, X. L. Tian, and D. J. Zeng, et al., Design and analyses of an ultra-thin flat lens for wave front shaping in the visible, Phys. Lett. A. 379 (2015) 3008-3012.